On the existence of a second phase transition in ferroelectrics with Aurivillius-type structure through the study of the Young's modulus

On the existence of a second phase transition in ferroelectrics with Aurivillius-type structure through the study of the Young's modulus

B Jiménez†, P Duran-Martín‡, R J Jiménez-Rioboo† and R Jiménez†

† Instituto de Ciencia de Materiales de Madrid, CSIC, Cantoblanco, 28049 Madrid, Spain
‡ Swiss Federal Institute of Technology, Materials Department, Ceramics Laboratory, 1015 Lausanne, Switzerland

Abstract. The possible existence of a second phase transition in Aurivillius-structure-type ferroelectric compounds is discussed. For this purpose, measurements of the complex elastic (Young's) modulus, dielectric constant, DC conductivity and Raman spectra as a function of temperature have been performed. The results suggest that the anomalies that appear in macroscopic complex elastic modulus, DC conductivity and, probably, those of the 25 cm^{-1} vibration mode of Raman spectra near the temperature of 300 °C do not correspond to a ferro-paraelectric or ferro–ferroelectric phase transition. Anomalies in the dielectric constant have only been found at the phase transition temperatures. Brillouin measurements show that the 300 °C anomaly is of extrinsic character, which could be connected to shallow point defects caused by the Bi^{3+} instability in the Bi_2O_2 layer. With increasing temperature, the defects are ionized increasing the DC conductivity and changing the elastic properties of the material by pinning domain walls or dislocations. Electron spin resonance (ESR) spectra, obtained after heating the samples at $T = 500$ °C, show the line of the almost free electron from the ionized defects.

1. Introduction

The interest of ferroelectric thin films for application in non-volatile memories and infrared sensors is continuously growing [1]. However, problems such as fatigue, aging, retention of polarization and the presence of lead in their compositions limit the use of classical compositions based on lead zirconate titanate. Thus, it becomes necessary to find new compositions that can overcome these problems.

Thin films of lead-free ferroelectric compositions [2, 3] that can meet such requirements are the ferroelectric layered perovskites sandwiched between Bi_2O_2 layers forming an Aurivillius-type crystalline structure, figure 1. The Aurivillius-type ferroelectric phases with high T_c are also very interesting as bulk materials for devices such as ultrasonic sensors, accelerometers etc to work at high temperatures. Many Aurivillius compositions with even number of perovskite-like layers between two Bi_2O_2 layers, such as Bi_3TiNbO_9 ($n = 2$) and $Bi_5Ti_3FeO_{15}$ ($n = 4$), exhibit two phase transitions 200 °C apart. Compositions with odd number of perovskite-type layers, such as $Bi_4Ti_3O_{12}$ (BTO), with $n = 3$, show only a single phase transition [4]. In view of this curious state of the art, the possibility of the existence of a second phase transition in compounds with $n = 3$ was considered. Raman spectroscopy results obtained in $n = 3$ Aurivillius compounds by following the evolution of certain lattice vibration modes as a function of the temperature [5, 6] make it possible to consider the existence of a phase
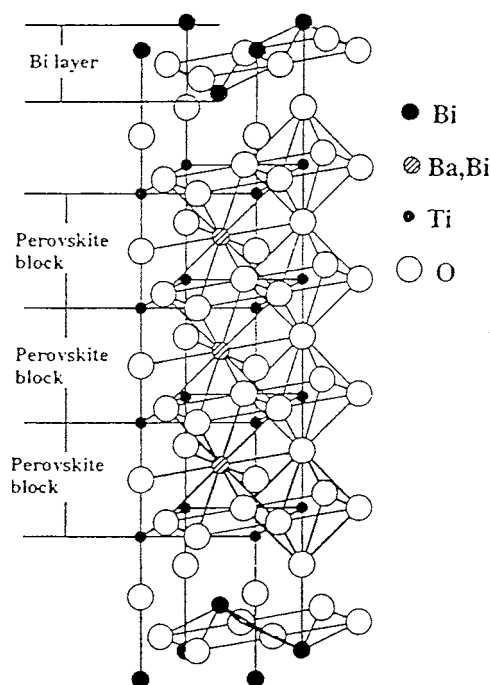
Figure 1. Aurivillius-type structure with even number ($n = 4$) of perovskite layers sandwiched by two layers of Bi_2O_2.

transition at such a temperature, showing a disappearance or an important change at about 300 °C. However, x-ray diffractograms and dielectric constant data do not show appreciable changes that could point to a structural phase transition at that temperature. In the even layer number Aurivillius ferroelectrics, the lower temperature phase transition is first order and also difficult to observe, and at higher temperature is a second order phase transition.

Concerning the second phase transition of the even n compounds, some of the reported results [7] look similar to those of the ferroelectrics with diffuse phase transitions where the ferroelectric polarization and birefringence disappear at temperatures much lower than that where the maximum of dielectric constant occurs [8].

It is known that the ferro–paraelectric phase transition can be effectively studied using measurements of the complex elastic modulus as a function of temperature with ultrasonic or lower frequency measuring methods, like the torsion pendulum and the three point bending technique [9]. These methods are very sensitive to changes in the coupling order parameter with the spontaneous strain [10] and to the interaction of point defects with larger defects such as domain walls, dislocations etc [11–13]. Previous low-frequency measurements of the Young's modulus in $n = 2$ Aurivillius phases reported by the present authors showed anomalies at temperatures close to 300 °C [14].

To ascertain the possible existence of a second phase transition, we have broadened the study to include compounds with even, odd and mixed number of perovskite layers. Different solid solutions are also studied. Low-frequency measurements of the complex Young's modulus as a function of the temperature were performed. In the study of some of the samples we have also used electrical measurements and optical spectroscopies (Raman and Brillouin). Comparison of the results here obtained from different techniques will give valuable information on the behaviour of the Aurivillius-type ferroelectrics.

2. Experimental procedure

Aurivillius structure compositions as shown in table 1 were obtained from oxide and carbonate mixtures with sintering performed at $1100\,^{\circ}$C. The preparation and sintering process yields microstructures where the largest faces of the plate-like grains (*c*-axis perpendicular to the largest face) of the ceramic are especially in planes perpendicular to the green pastille forming pressure and randomly distributed. The obtained ceramics have a densification of 95–96%. The used samples were cut perpendicular to the largest faces of the ceramics.

Table 1. List of the different compositions studied in the present work, indicating their *n* and *m* numbers of perovskite layers, the abbreviated name used in this work and their corresponding T_c.

Composition	*n*	Name	*m*	T_c ($^{\circ}$C)
$Bi_2SrNb_2O_9$	2	(SBN)	0	420
Bi_3TiNbO_9	2	(BTN)	0	930
$(Bi_2SrNb_2O_9)_{0.25}(Bi_3TiNbO_9)_{0.75}$	2	(SBN25BTN75)	0	810
$(Bi_2SrNb_2O_9)_{0.50}(Bi_3TiNbO_9)_{0.50}$	2	(SBN50BTN50)	0	680
$Bi_{1.50}Te_{0.50}Sr_{0.50}Na_{0.50}Nb_2O_9$	2	(SNBTeN50)	0	400
$Bi_{1.75}Te_{0.25}Sr_{0.75}Na_{0.25}Nb_2O_9$	2	(SNBTeN25)	0	350
$CaBi_4Ti_4O_{15}$	4	(CaBTO)	0	780
$PbBi_4Ti_4O_{15}$	4	(PbBTO1)	0	560
$Pb_2Bi_4Ti_5O_{18}$	5	(PbBTO2)	0	310
$Pb_3Bi_4Ti_6O_{21}$	3	(PbBTO3)[a]	2	200

[a] The last compound has a mixed structure, i.e. there are layers of 3 (*n*) and 2 (*m*) perovskite layers sandwiched between Bi_2O_2 layers.
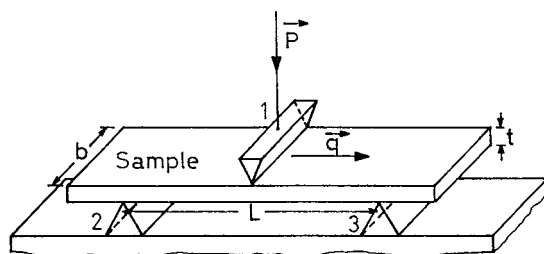

Figure 2. Schematic diagram of the TBP measuring technique, where: P = stress, q = wavevector, L = effective length, t = thickness, b = width.

Concerning the compositions with substitutions in the Bi_2O_2 layer, SBNTeN$_x$ (x = 0, 0.25, 0.50), it was generally believed that chemical modification of the layer was forbidden [15]. However it has been proved [16] that cations with a stereochemically active lone pair of electrons, such as Pb^{2+}, Sb^{3+} or Te^{4+}, can replace Bi^{3+} without altering the basic structure.

Several experimental techniques were used to obtain information on macro or microscopic physical parameters that undergo changes in the structural phase transition temperature.

The Young's modulus as a function of the temperature was obtained by a low-frequency (1 Hz) dynamic mechanical analysis (DMA) based on the three point bending technique (TPB), figure 2, at a heating and cooling rate of $1\,^{\circ}$C min^{-1}. Samples of $12.0 \times 2.0 \times 0.4$ mm^3 dimension were used.

Electrical impedance measurements as a function of temperature at different frequencies (1 kHz–1 MHz) were performed on thin (0.5–1 mm) samples of 9.0 mm diameter. From these
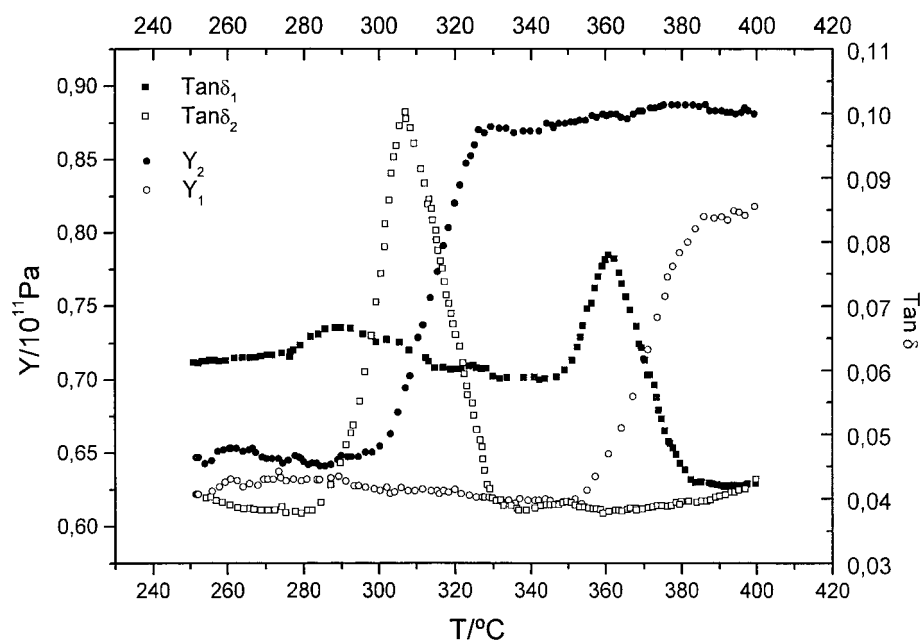
Figure 3. Young's modulus and tan δ as a function of the temperature for SBN ($n = 2$) sample, (1) first run, (2) after seven days.

measurements, DC conductivity from extrapolation of complex impedance arcs and dielectric constant were obtained.

Micro-Raman spectroscopy measurements were performed in the Raman Laboratory of the Experimentalphysik Institute of the University of Saarland in Germany.

Brillouin spectroscopy (BS) was performed on a 3+3 in tandem Fabry–Pérot interferometer (J Sandercock [17]) using the backscattering geometry. Full description of the experimental set-up can be found in [18].

Electron spin resonance (ESR) spectra were obtained at the liquid N_2 temperature in non-treated and 500 °C thermally treated samples.

3. Experimental results

In figure 3, the variation of the Young's modulus, Y, and mechanical losses, tan δ, as a function of the temperature are plotted for sample SBN. The curve shows a strong jump in the Young's modulus and a peak in mechanical losses at 355 °C in the first heating run and similar anomalies at 300 °C in the second heating run that was obtained seven days after the first one.

In figure 4, we have plotted the thermal behaviour in the first heating run of the Young's modulus for sample CaBTO ($n = 4$), and for the solid solutions SBN25BTN75 and SBN50BTN50 ($n = 2$). In all of these samples the modulus Y shows a clear increase which starts at 300 °C.

Measurements of Y-modulus in lead-containing compositions, PbBTO1 ($n = 4$), PbBTO2 ($n = 5$) and PbBTO3 ($n = 3$, $m = 2$) are plotted in figure 5. Anomalies are observed at temperatures close to 300 °C for the PbBTO1 and PbBTO3 samples in the heating runs but not in the cooling ones. The sample PbBTO2 does not show an additional anomaly at 300 °C probably due to the large change of Y accompanying the ferro–paraelectric phase transition.
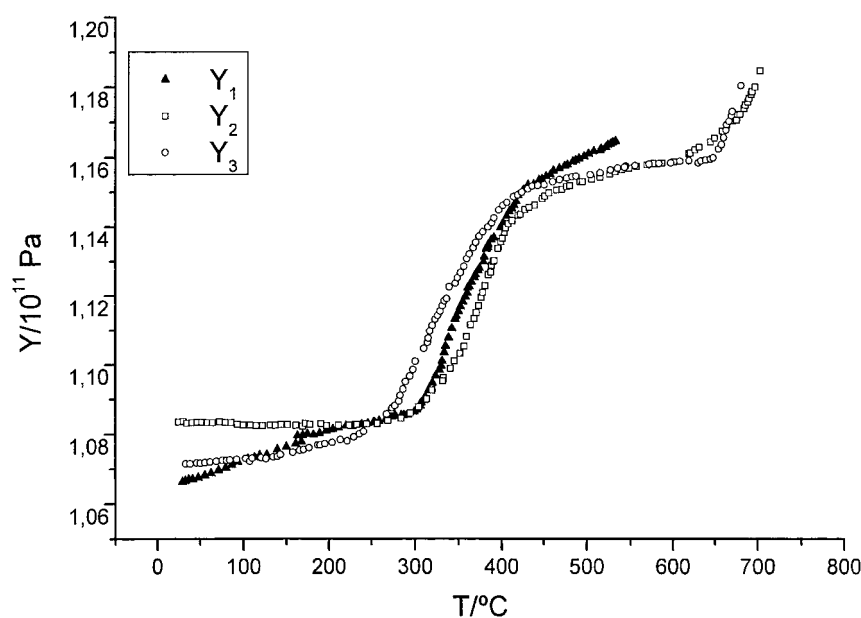
Figure 4. Young's modulus as a function of the temperature, SBN25BTN75 ($n = 2$) (Y_1), SBN50BTN50 ($n = 2$) (Y_2) and CaBTO ($n = 4$) (Y_3) samples.

The dielectric constant of PbBTO2 as a function of the temperature shows diffusive character with a maximum of ε' at $T = 300\,°C$, figure 6.

In all samples studied, the anomaly close to $300\,°C$ does not appear in the cooling runs, i.e. it shows an irreversible behaviour. The temperature of this anomaly does not correspond to the ferro–paraelectric phase transition temperature of the studied compositions. In table 1 the temperature of the dielectric constant maximum for each composition at the frequency of 10 kHz is listed. Only one maximum for each composition was observed. This behaviour leads us to think that we are not dealing with a structural phase transition, because the anomaly appearing in the structural phase temperature, as due to the coupling between the order parameter and the spontaneous strain [10] is always reversible.

Most of the studied samples show colour changes from dark grey at room temperature to pale yellow at temperatures close to $400\,°C$. This behaviour suggests modifications in the defect structure of the material at certain temperature that must be reflected in the behaviour of the electrical conductivity as a function of the temperature. Figure 7 shows the Arrhenius plot of the DC conductivity obtained from complex impedance arcs in the sample of composition $(SBN)_{0.50}(BTN)_{0.50}$. The curve presents two well defined slopes: below $340\,°C$ the value of the slope is 0.73 eV; in the interval $440–580\,°C$ the slope reaches the value of 3.41 eV. A wide thermal hysteresis in the conductivity is also observed. Similar qualitative behaviour is reported in Nb-doped BTO by Shulman *et al* [19] and the solid solution $(SrBi_2Ta_2O_9)_{1-x}(Bi_3TiNbO_9)_x$ shows changes in the slopes of the Arrhenius plots at temperatures close to $300\,°C$ over the complete range of solution [20], but only heating runs were studied and no thermal hysteresis or reversibility were reported.

It is worth emphasizing that the change in the slope of the DC conductivity and the jump in the elastic modulus take place at quite close temperatures. This suggests that some mechanism related to defect centres and their environment is responsible for the obtained electric and elastic response.
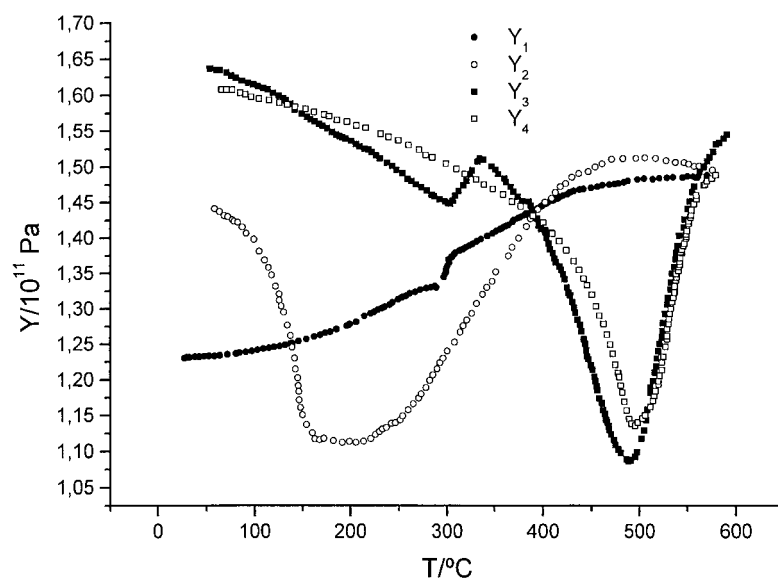
Figure 5. Young's modulus as a function of the temperature for PbBTO1 (Y_1), PbBTO2 (Y_2) and PbBTO3 (Y_3) samples on heating. Y_4 corresponds to the PbBTO2 sample on cooling.
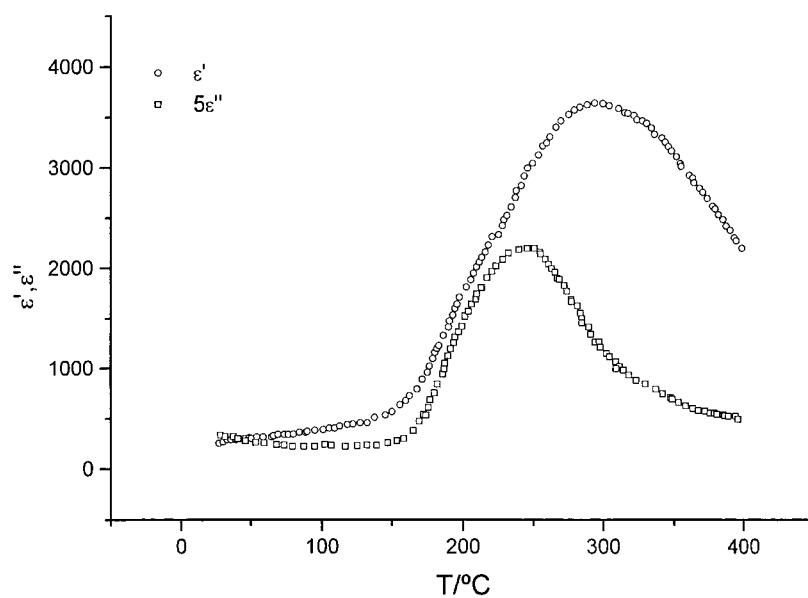

Figure 6. Dielectric constant, ε', and dielectric losses, ε'', as a function of the temperature for PbBTO2 sample.

Modifications in the defect centres and their environment can be studied by Raman and ESR spectroscopies because of the sensitivity of the technique to changes in the structural and electrical conditions of these centres. In the Raman spectra we have observed the thermal evolution of some low-frequency vibration modes (25–30 cm^{-1}) in SBNTeN25 samples, figure 8. The peak corresponding to the 30 cm^{-1} vibration mode disappears or becomes very small and broad at a temperature close to 300 °C. The disappearance of vibration modes
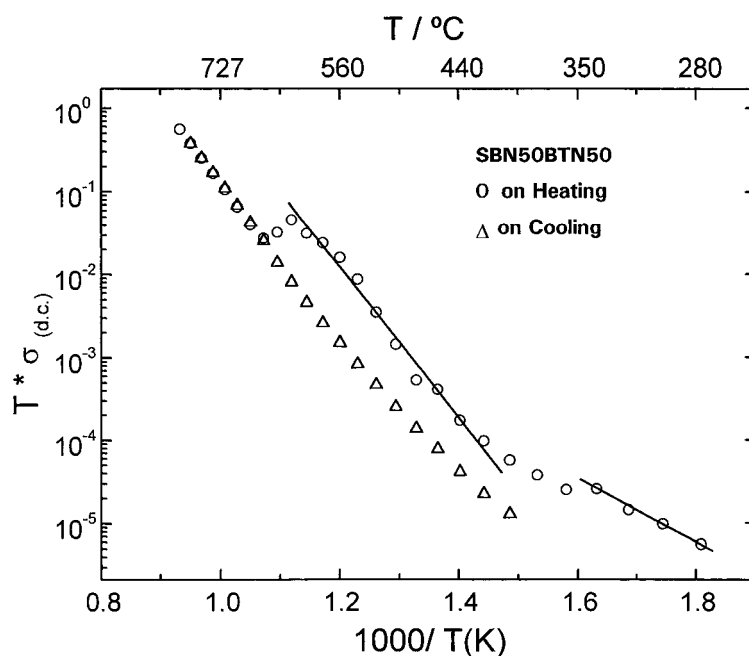
Figure 7. Arrhenius plot of DC conductivity for SBN50BTN50 sample. The lines indicate slopes below 340 °C and in the range 440–580 °C.

of the same frequencies at similar temperatures has been observed in many other Aurivillius-type compounds. The most noteworthy, $Bi_4Ti_3O_{12}$ (BTO) [21], exhibits a 25 cm^{-1} vibration mode that disappears at temperatures which depend on the grain size. For a 100 nm grain size the disappearance of the vibration mode occurs at the temperature of 330 °C. Recently, Raman studies on $Bi_2SrTa_2O_9$ (SBT) [22] have shown that a 26 cm^{-1} vibration mode disappears at the temperature of 272 °C, while the transition temperature is 335 °C.

Figure 9 shows the ESR spectra for samples SBN and BTN, the extreme compositions of the solid solution $(SBN)_x(BTN)_{1-x}$, obtained at the temperature of the liquid N_2 before thermal treatment (dashed curves), and after a treatment at 500 °C for 15 min (solid curves). Resonance lines at $g = 2.0024$ are observed only in thermally treated samples. The g value is very close to that of the free electron. Thus, it seems clear that the heat treatment has modified the state of electrical charge of the defect.

It is convenient for the aim of this study, to distinguish if the elastic anomalies are of extrinsic or intrinsic character. For this purpose we make use of Brillouin spectroscopy which provides information about the intrinsic elastic properties by studying the evolution of the acoustic phonons after thermal treatment of the sample. The obtained spectra for the composition SBNTeN25 are shown in figure 10. Due to the microstructure of the ceramic, the peaks corresponding to both the transverse and longitudinal phonons were present in the backscattering spectra. The observed double peak structure is due to the existence of preferential orientation of the grains in the ceramic sample. After the first measurement, curve (b), the sample was heated up to 650 °C and left free to cool down to obtain the curve (a). The results do not show significant changes in the positions of the characteristic peaks in both spectra that could suggest structural modifications. This means that the high-frequency elastic properties are reversible and of intrinsic character. The calculated Young's modulus (115 GPa) is higher than that for low frequency (80 GPa) obtained from measurements with the
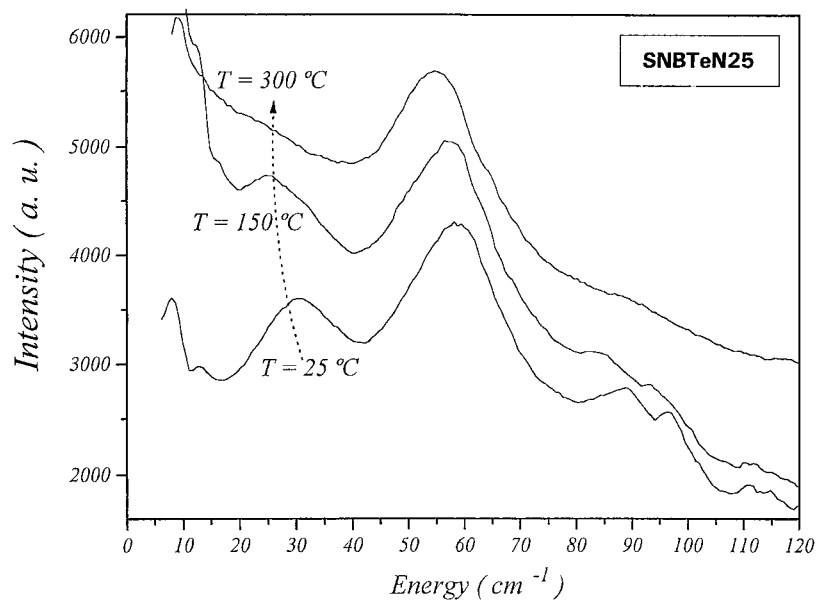
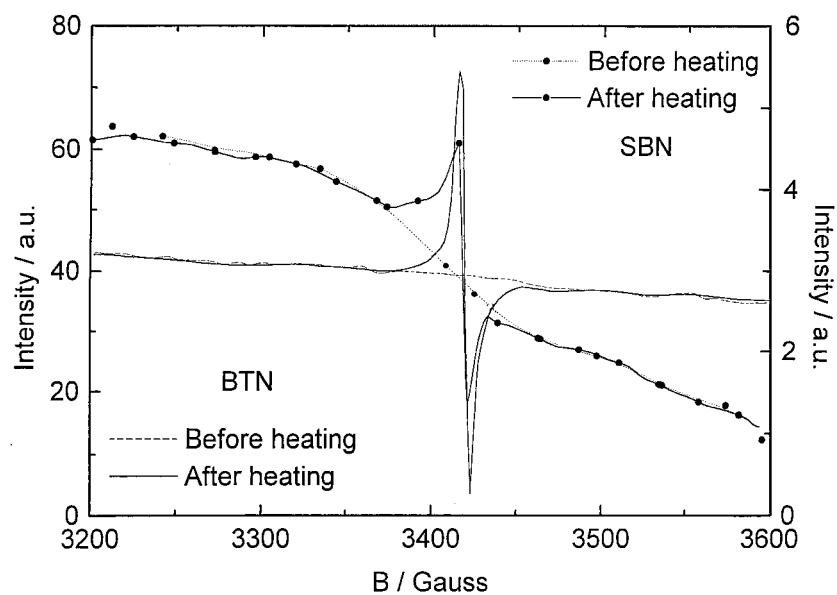**Figure 8.** Raman spectra at different temperatures for the sample SNBTeN25.

Figure 9. ESR spectra for non-treated (———) and 500 °C (- - - -) treated SBN and BTN samples.

TPB method for SBNTeN25. The difference between the high- and low-frequency values of the Young's modulus suggests the existence of an extrinsic mechanism of low-frequency dispersive character that the Brillouin spectroscopy is not able to see. If the relationship between the frequency of the spectroscopy, ω_{BS}, and the relaxation time of the studied mechanism, τ_{LF}, is $\omega_{BS}\tau_{LF} > 1$, the spectroscopy does not give information on such a mechanism [9]. In the actual case, $\omega_{BS} \cong 10$ GHz, $\tau_{LF} > 10^{-4}$ s [11–13], and the above condition is accomplished.
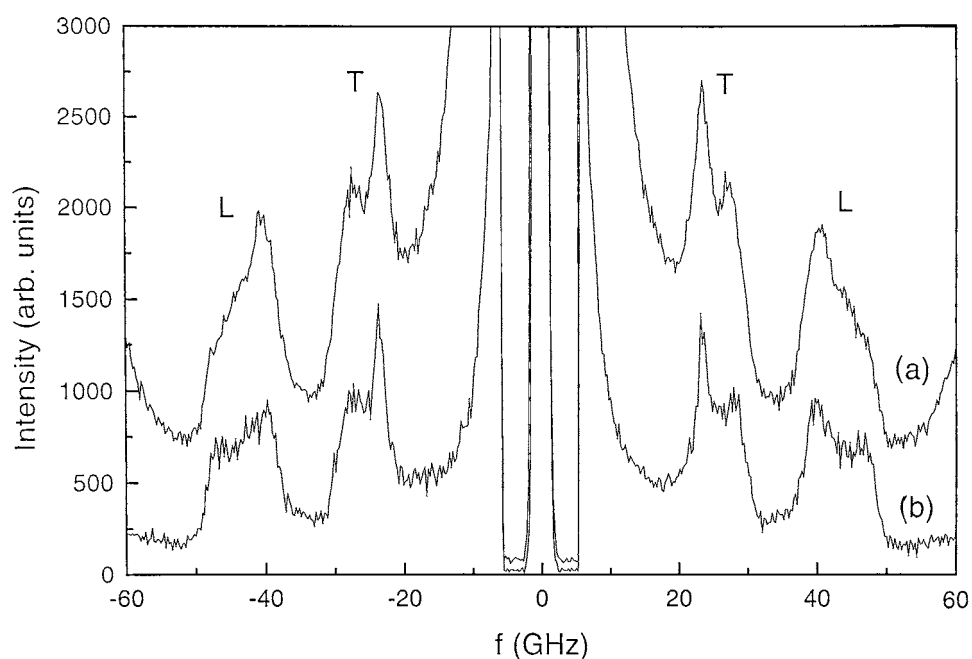
Figure 10. Brillouin spectra for 650 °C treated (a) and non-treated (b) SBNTeN25 sample.

4. Discussion

The thermal behaviour of the Raman vibration modes, DC electrical conductivity and low-frequency elastic modulus present a sort of 'magic' temperature, around 300 °C, where anomalies appear in all the studied compositions. The lack of reversibility in the heating–cooling cycle and x-ray studies clearly indicate that there is no structural phase transition as reported by other authors [21]. The observed behaviour must most likely be related to the Bi_2O_2 layer that is the common compositional entity present in all the studied compositions.

Data obtained from x-ray and neutron diffractograms do not support the existence of a low-temperature phase transition. The most significant studies have used Raman spectroscopy because it is very sensitive to local structural changes. In the case of BTO [21] the authors attribute the observed behaviour of the 25 cm^{-1} mode to an electron instability in the Bi^{3+} ion, that results in a transfer of electrons from the Bi^{3+} lone pair of electrons to the empty 3d orbital of the Ti^{4+} cation via the oxygen ions. This charge transfer is considered as a bridge in the Bi–O–Ti system with an effective transfer of charge to and from Bi–O and Ti–O bonds. Such a bridge was used to explain the ferroelastic phase transition observed in $BiVO_4$ [23]. Therefore, the above authors [21] associate the behaviour of the 25 cm^{-1} vibration mode (soft mode) with a ferroelectric phase transition in BTO at 330 °C, in addition to the well known ferro–paraelectric transition for this compound taking place at 675 °C. However, no changes in x-ray diffraction were found at 330 °C that could confirm a new structural phase transition.

According to the low-frequency and Brillouin spectroscopy results, the mechanism causing the observed anomalies must have a dynamical character with a very high relaxation time. Low-frequency relaxational mechanisms in materials have, generally, an extrinsic origin and usually come from thermal diffusion of defects, thermal fluctuations, cationic disorder etc [9, 11]. It should be borne in mind that chemical composition and preparation processes of the

studied ceramics create a high point defect concentration by lack of stoichiometry or changes in the cation site position. Supporting this idea there are recent studies [24, 25] which propose that some of the limitations of the lead-free Aurivillius compositions for thin films with good characteristic for memory applications would come from the instability of the Bi^{3+} cation that diffuses to the surface of the films when the temperature increases. It is also reported [25] that holes trapped in Bi^{3+} or electrons trapped in Ta^{5+} will form Bi^{4+} and Ta^{4+} shallow centres with low activation energy.

The ESR spectra of figure 9 suggest that an imbalance of charge is produced by a simple thermal treatment: before treatment the defect is not paramagnetic, it is not ionized and the initial dark colour of the material should probably come from a high concentration of oxygen vacancies. These results could confirm the existence of the above mentioned shallow centres.

A certain disorder in the perovskite slabs in some Aurivillius-type structure compounds has been determined by the combined use of x-ray and neutron powder diffraction [26] with mixing of Bi and A-site cations on their respective sites. This disorder can also produce charged point defects by lack of stoichiometry and charge balance in the Bi/Sr–O–B systems.

It is well accepted that there exists an important positional instability in the Bi^{3+} cation that could give place to defects like cation or oxygen vacancies, but it is not clear from which structural site it comes. Studies of the electronic structure of Bi_2NbO_6 ($n = 1$) [27] have shown that the Bi_2O_2 layer is the main source of oxygen vacancies in this compound. The slight differences in the temperature and height of the jump in the studied materials suggest that the anomalies have a common origin and it is evident that the common entity in all the compositions is the Bi_2O_2 layer.

To see how the point defects influence the elastic constants we give an approach without taking into account structural, microstructural or textural aspects of the material. A simple model is taken where calculations are made by considering an atomistic nearest-neighbour force-constant description [28].

In the model it is assumed that the atoms are connected by springs. The introduction of point defects will change certain springs that modify the average over all the springs and, consequently, the elastic properties will change.

Let us consider a monatomic solid with N atoms, p_i springs of type i and strength f_i attached to each atom. If a small fraction, c, of all the atoms is replaced, the cNp_i springs will have changed their strength by Δf_i and the averaged force constant becomes:

$$\Delta f = f_i(1 + 2c\Delta f_i/f_i). \tag{1}$$

When the defect is a vacancy, we take $\Delta f_i = -f_i$ and obtain

$$f_{av} = f_i(1 - 2c). \tag{2}$$

In the case of an fcc lattice with only nearest-neighbour central interactions, the force constants attached to a substitutional defect change from f to $f + \Delta f$. Calculations of the changes in the elastic constants as performed in [29] and [30] deliver the following expressions:

$$\Delta(c_{11} - 2c_{12})/(c_{11} - 2c_{12}) = 2c(\Delta f/f)(1 + 0.38\Delta f/f)^{-1} \tag{3}$$

$$\Delta(c_{11} + 2c_{12})/(c_{11} + 2c_{12}) = 2c(\Delta f/f)(1 + 0.24\Delta f/f)^{-1} \tag{4}$$

$$(\Delta c_{44})/c_{44} = 2c(\Delta f/f)(1 + 0.33\Delta f/f)^{-1}. \tag{5}$$

For a vacancy, $\Delta f/f = -1$. Thus, the relative changes of the elastic constants c_{ij} should be of the order of $3c$.

In an isotropic system the shear modulus takes the value of the stiffness coefficient c_{44}

$$G = c_{44} = 1/s_{44} \tag{6}$$

and the Young's modulus will be:

$$Y = 2G(1 + \nu) = 2c_{44}(1 + \nu) \tag{7}$$

where ν is the Poisson coefficient. Therefore, the variation of the modulus Y with the vacancy concentration takes the form:

$$\Delta Y/Y = \Delta c_{44}/c_{44} = -3c. \tag{8}$$

Thus, it is deduced that when the substitute atom is less stiff than those of the host material, the Young's modulus decreases.

A relation between the concentration of point defect (vacancies or atoms) and the change of the Young's modulus at the temperature close to 300 °C in Aurivillius-type ceramics was pointed out in [14]. In that case, measurements in compositions with different proportion of Bi/Te substitution show that the larger the amount of substituted Bi, the smaller the increase of the Young's modulus. According to [16], the Te substitutions for Bi in SBN (strontium–bismuth niobate) decrease the amount of oxygen vacancies in the compound.

The influence of oxygen vacancies on the elastic properties of the materials has been proved from low-frequency measurements of elastic moduli in Cu–Zn alloys [31–34] quenched from 800 °C. It is found that the internal friction coefficient presents a peak at 240 °C in the heating run and at 50 °C in the cooling one. This behaviour is attributed to the high concentration of oxygen vacancies trapped in dislocations and other extended defects during quenching. After the first heating, the number of vacancies decreases considerably.

In the second heating of the studied ceramics, performed immediately after the first one, the Young's modulus does not present an anomaly at temperatures close to 300 °C. It is necessary to wait for a long time (days) to recover an important jump at lower temperature than that obtained in the first heating, see figure 3. This result suggests a large change in the state or number of centres causing the anomaly.

In ferroelectric materials the point defects, mainly oxygen vacancies, are pinning the 90° domain walls and the Young's modulus shows a relaxation at frequencies of 1–3 Hz [11–13] and a temperature of 150 °C. Thus, it is verified that the existence of point defects clearly affects the low-frequency elastic modulus behaviour. In the present study, the Young's modulus presents non-reversible anomalies at temperatures around 300 °C that cannot be attributed to structural phase transitions. Thus, we have to claim mechanisms different from those of the elasto-electrical coupling that take place in the ferro–paraelectric phase transition to explain the obtained experimental results. In the results obtained for the PbBTO$_3$ sample the anomaly appears above the ferro–paraelectric phase transition temperature, figure 5, and could confirm the participation of vacancies and other extended defects in the anomaly of the elastic properties. A plausible mechanism would consist of the modification of complex defects formed, probably, by oxygen vacancies and antisite cations due to the stoichiometric disorder indicated in [26]. This process should take place at about 300 °C with later migration of vacancies and increases of the electrical conductivity and activation energy [35].

From the above considerations, it can be assumed that the main cause of the low-frequency Young's modulus behaviour that we have found in this work has an extrinsic character. The migration of charged point defects and their capture in other extended defects such as dislocations or domain walls increase the stiffness [36] of the sample. The change of the slope in the Arrhenius plot of conductivity and the jump in Young's modulus, that takes place in the temperature range of 300–350 °C, seems to confirm that the defects and their charge state should be responsible for the obtained experimental results. The main origin of such defects, apart from the stoichiometric disorder, is, probably, related to the instability of the Bi cations in the Bi$_2$O$_2$ layer, where oxygen vacancies are more easily created [27].

5. Conclusions

We report for the first time an anomaly in the Young's modulus at the temperature of 300 °C in compounds with Aurivillius-type structure.

A second phase transition, different from the ferro–paraelectric one for each composition, was not observed in any (having even or odd number of perovskite layers) of the studied samples. The absence of thermal reversibility in the measured parameters supports this conclusion.

The 300 °C anomalies that are observed in the heating runs of the Young's modulus, electrical conductivity and, probably, in the Raman vibration mode have an extrinsic character.

The cause of the above mentioned anomalies must be found in the electrical charge state of the point defects of the different compositions.

The main point defect present must be the cation or oxygen vacancy coming from instability of the Bi^{3+} cation in the Bi_2O_2 layer.

References

[1] Scott J F 1998 *Ferroelectr. Rev.* **1** Monograph
[2] Paz de Araujo C A, Cuchiaro J D, McMillan L D, Scott M C and Scott J F 1995 *Nature* **374** 627
[3] Isai H M, Lin P and Tseng T Y 1998 *Appl. Phys. Lett.* **72** 1787
[4] Newnham R E, Wolfe R W, Horsey R S, Díaz-Colón A and Kay M I 1973 *Mater. Res. Bull.* **8** 1183
[5] Cummins S E and Cross L E 1968 *J. Appl. Phys.* **39** 2268
[6] Rae A D, Thomson J G, Withers R L and Willis A C 1990 *Acta Crystallogr.* B **46** 474
[7] Newnham R E, Wolfe R W, Horsey R S and Díaz-Colón F A 1973 *Mater. Res. Bull.* **8** 1183
[8] Smolensky G A 1970 *J. Phys. Soc. Japan* **28** 26
[9] Kytik A V, Schranz W, Fuith A, Havlik D, Sporonyuk V P and Warhanek H 1996 *Phys. Rev.* B **53** 3055
[10] Rehwald W 1973 *Adv. Phys.* **22** 721
[11] Gridnev S A 1990 *Ferroelectrics* **112** 107
[12] Chen B L, Gabbay M and Fantozzi G 1996 *J. Mater. Sci.* **31** 4141
[13] Jiménez B and Vicente J M 1998 *J. Phys. D: Appl. Phys.* **31** 446
[14] Jiménez B, Durán-Martín P, Jiménez R J and Jiménez R 1999 *J. Eur. Ceram. Soc.* **5**
[15] Subbarao E C 1962 *J. Am. Ceram. Soc.* **45** 166
[16] Ramirez A, Millán P, Castro A and Torrance J B 1994 *Eur. J. Solid State Inorg. Chem.* **31** 173
[17] Sandercock J R 1982 *Light Scattering in Solids III (Topics in Applied Physics 51)* (Berlin: Springer) ch 6
[18] Jiménez-Rioboo R J, García-Hernández M, Prieto C, Fuentos-Gallego J J, Blanco E and Ramírez-del-Solar M M J 1997 *J. Appl. Phys.* **81** 7739
[19] Shulman H S, Testorf M, Damjanovic D and Setter N 1996 *J. Am. Ceram. Soc.* **79** 3124
[20] Zhu Y, Zhang X, Gu P, Joshi P C and Desu S B 1997 *J. Phys.: Condens. Matter* **9** 10 225
[21] Meng J, Huang Y and Zou G 1996 *Solid State Commun.* **97** 887
[22] Kojima S 1998 *J. Phys.: Condens. Matter* **10** L327
[23] David W L F 1983 *J. Phys. C: Solid State Phys.* **16** 5127
[24] Scott J F *Abs. EMIF2 (Juy-en-Josas, 1997)* PC.1
[25] Robertson J, Chen C W, Warrenand W L and Gutleben C D 1996 *Appl. Phys. Lett.* **69** 1704
[26] Blake S M, Falconer M J, McCreedy M and Lightfoot P 1997 *J. Mater. Chem.* **7** 1609
[27] Medvedeva N I, Turzhevsky S A, Gubanov V A and Freeman A J 1993 *Phys. Rev.* B **48** 16 061
[28] Grimwall G 1986 *Thermophysical Properties of Materials* ed E P Wohlfarth (Amsterdam: North-Holland) ch 6, p 141
[29] Dederichs P H and Zeller R 1980 *Point Defects in Metals II* (Berlin: Springer)

[30] Leibfried G and Breuer N 1978 *Points Defects in Metals I* (Berlin: Springer)
[31] Van Humbeek J and Delaey L 1983 *J. Physique Coll.* **12** C9 217
[32] Bojarski Z, Ilzuk J, Panek T and Marawiec H 1983 *J. Physique Coll.* **12** C9 241
[33] Hausch G, Schmolz A, Török E and Warlimont H 1983 *J. Physique Coll.* **12** C9 471
[34] Wolten G M 1963 *J. Am. Ceram. Soc.* **46** 418
[35] Yang F, Wang Y, Liu J, Zhang Z and Chen X 1999 *Appl. Phys. Lett.* **74** 2794
[36] Schaefer H E, Damson B, Weller M, Arzt E and George E P 1997 *Phys. Status Solidi* a **160** 531